



Interfaces and Surfaces Analyses Service

## Interfaces and Surfaces Analyses Service

### Identity

#### Composition of the team (or participants)

Team leader: E. Beche (IR)  
Permanent personnel : D. Perarnau (AI)

#### Keywords

Multi-scale characterization, microstructural modelization, materials properties, quality management system

---

#### Topics

##### 1. Technical projects

Determination of instrumental function and experimental sensitivity factors  
Chemical and physical effects of excitation sources: Artifacts and modifications of signal

##### 2. Scientific projects

Qualification of LCZO compounds elaborated with solar energy  
Investigation of Sr-substituted lanthanum manganite perovskites  
Investigations of oxidized ZrB<sub>2</sub>-SiC fiber compounds elaborated at high temperature with solar energy

#### Collaborations

##### National

- V. Flaud (ICGM, Montpellier) ; S. Roualdès (IEM, Montpellier) ; V. Rouessac (IEM, Montpellier) ; Van der Lee (IEM, Montpellier) ; J. Esvan (CIRIMAT-ENSIACET, Toulouse) ; T. Duguet (CIRIMAT-ENSIACET, Toulouse) ; P. Fau (LCC, Toulouse) ; F. Berger (LCE, Besançon).

##### International

- L. Mercatelli (CNR-INO, Firenze, Italia) ; E. Sani (CNR-INO, Firenze, Italia) ; D. Sciti (ISTEC-CNR, Faenza, Italia) ; D. Alfano (CIRA, Capua, Italia) ; O. Levasseur (Dpt Phys. Montreal, Canada) ; L. Stafford (Dpt Phys. Montreal, Canada)

##### Some contracts (7/18)

- MSFI (project), Coordinator ; IMSI (project), Coordinator ; LCZO (project), Coordinator ; T3 – WP13 – SFERA (project), Coordinator ; ECHREF (project), partner ; PEROVSKITE (project), partner ; UHTC (project), partner

#### Large equipment

- XRD diffractometer MPD X' Pert PRO ( $\theta-\theta$ ), (PANalytical, 2011), laboratory and SFERA funding source
- XPS-AES techniques, (RIBER-CAMECA spectrometer, 1987-1992), laboratory funding source
- IR-TF spectrometer Nexus 670, (NICOLET, 2001), laboratory funding source

## Scientific report

### INTRODUCTION

Since 2001, SASI is an analyses department of PROMES laboratory. Microstructural analyses are performed with XPS, AES, XRD, FT-IR techniques.

Missions:

- To achieve a high level of professionalism in our studies (microstructure and material properties).
- To provide a high level of training in the field of materials characterization.

Department policy

- To guarantee reliability and traceability of results.
- To guarantee capitalization and sharing of expertise to the laboratory.
- To ensure the people's training of our service and partner's departments.
- To guarantee scientific communication of our studies in scientific conference and technical workshop.

Objectifs :

- Optimization and development of analytical experiments and methods.
- Collaboration in scientific activities (national and international projects of PROMES lab.)
- Development of technical training for users..

### 1. TECHNICAL PROJECT

Permanent personnel : D. Perarnau, E. Beche

Partner: V. Flaud (ICGM, Montpellier), J. Esvan (CIRIMAT, Toulouse)

Project: MSFI (Determination of instrumental function of spectrometer and experimental sensitive factors)

Project: IMSI (Identification of modifications on irradiated surfaces)

The qualification of new materials requires multi-scale characterization techniques. In order to optimally correspond to these requirements, analyses were performed on devices of our laboratory and in collaboration with other analyses service.

Objectives:

- To develop and provide analytical methods and processes using for devices operating with the same technique (comparative studies). (MSFI project)
- To select and optimize experimental parameters for reference samples and use dashboard of optimized parameters for all compounds in order to provide a high quality of data and signal. (IMSI projects)
- To define documents (procedures, operating manuals, user guide...) for quality system (QSM) for all partners (MSFI and IMSI projects).

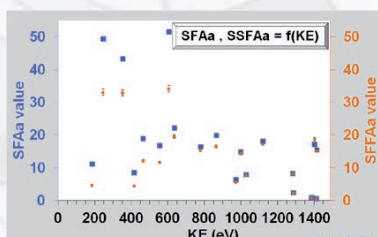


Figure 1 : Calculated (SFFAa) and theoretical (SFAa) sensitive factors v.s. kinetic energy of the photoelectrons (EK).

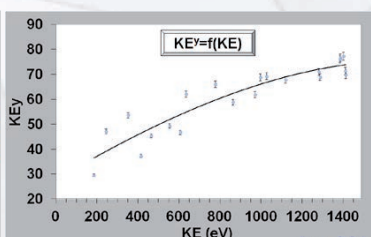


Figure 2 : Instrumental function of spectrometer (KEY) v.s. kinetic energy of the photoelectrons (EK).

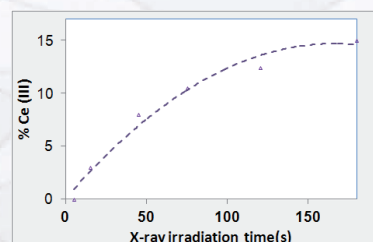


Figure 3 : Ce(III) species induced under X-ray irradiation of the surface of CeO<sub>2</sub> compound.

These technical studies are all necessary to guarantee to the users the reliability of the chemical and physical results collected for each technique.

## 2. SCIENTIFIC PROJECTS

Our objectives are to establish relationship between the microstructure, the chemical and physical properties and the experimental parameters of elaboration or surface treatment of compounds. A multi-scale characterization approach (nanoscale to microscale) was performed using several methods and techniques. Relevant results are obtained for mixed oxides.

### 2.1. Investigations of LCZO compounds elaborated by solar energy

Permanent personnel : D. Perarnau, E. Beche, G. Peraudeau (co-responsible)  
Partner : V. Flaud (ICGM, Montpellier)  
Project : **LCZO** (LaZrCeO)

Previous studies revealed promising properties of LCZO compounds in particularly for  $\text{La}_{0.8}\text{Ce}_{1.2}\text{Zr}_2\text{O}_{7.6}$  chemical composition (pyrochlore to fluorite phase transition, E. Beche and al, Surf. Interface Anal.,44 (2012) 1045-1050).

Our objectives were to elaborate  $\text{La}_{0.8}\text{Ce}_{1.2}\text{Zr}_2\text{O}_{7.6}$  compounds under  $\text{H}_2$  atmosphere in order to highly increase the amount of  $\text{Ce}^{3+}$  species in this compound and to determine the ionic states of Ce atoms.

The  $\text{La}_{0.8}\text{Ce}_{1.2}\text{Zr}_2\text{O}_{7.6}$  compounds were elaborated from commercial powders ( $\text{CeO}_2$ ,  $\text{La}_2\text{O}_3$ ,  $\text{ZrO}_2$  Strem Chemical 99.9%) in air and in  $\text{H}_2$  atmosphere at the focus of a 2 kW solar furnace.

The diffractogram ( $\text{H}_2$ , fig.4) is attributed to a pyrochlore structure (face-centred lattice, space group Fd-3m). This structure is clearly identified by the two (331) and (511) diffraction peaks located at  $2\theta=27.37^\circ$  and  $2\theta=43.51^\circ$ , respectively. This compound ( $\text{H}_2$ ) is an oxygen-deficient solid solution but an ordered defect structure with 1/8 of the anions missing. For sample (air, fig.4), the intensities of the (331) and (511) diffraction peaks decrease due to the presence of a fluorite like-structure. This crystal structure is a disordered structure in which some of oxygen vacancies are filled.

3 final states of  $\text{Ce}^{4+}$  species ( $\text{Ce}3d^{9/4f^2} \text{O}2p^4$ ,  $\text{Ce}3d^{9/4f^1} \text{O}2p^5$ ,  $\text{Ce}3d^{9/4f^0} \text{O}2p^6$ ) and 2 final states of  $\text{Ce}^{3+}$  species are detected ( $\text{Ce}3d^{9/4f^2} \text{O}2p^5$ ,  $\text{Ce}3d^{9/4f^1} \text{O}2p^6$ ) (fig.6). The calculated Ce(III) states (green components, fig.5-6) are in the range of 3.8% (air) to 25.2% ( $\text{H}_2$ ) for about 7.5% of Ce total content. These values are corrected by the amount of induced Ce (III) due to X-ray exposure.

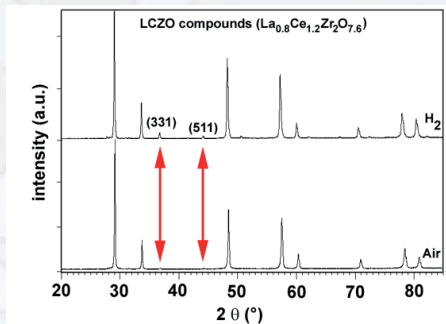


Figure 4 : Diffractograms collected for  $\text{La}_{0.8}\text{Ce}_{1.2}\text{Zr}_2\text{O}_{7.6}$  compounds elaborated under  $\text{H}_2$  and air.

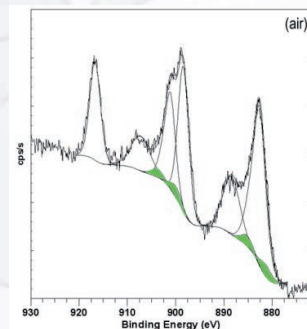


Figure 5 : Ce 3d3/2,5/2 XP-spectra collected for  $\text{La}_{0.8}\text{Ce}_{1.2}\text{Zr}_2\text{O}_{7.6}$  compounds elaborated under air

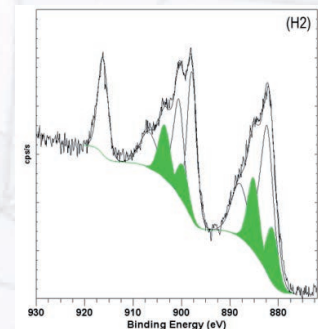


Figure 6 : Ce 3d3/2,5/2 XP-spectra collected for  $\text{La}_{0.8}\text{Ce}_{1.2}\text{Zr}_2\text{O}_{7.6}$  compounds elaborated under  $\text{H}_2$

## 2.2. Investigation of Sr-substituted lanthanum manganite perovskites

Permanent personnel : E. Beche, A. Demont, D. Perarnau, S. Abanades (Responsable du projet)

Partner : V. Flaud (ICGM, Montpellier)

Project : **PEROVSKITE**

Collaboration : Airbus Group Corporate Foundation (CNRS CT 084210) et CNRS (défi ENRS, VALTHER-CO2)

In the literature, the  $Mn^{4+}/Mn^{3+}$  redox couple is predicted to be thermodynamically inert toward  $CO_2$  oxidation within stoichiometric oxides such as the  $MnO_2/Mn_2O_3$  redox pair. Even the  $Mn^{3+}/Mn^{2+}$  redox couple is inactive in simple manganese oxides ( $Mn_3O_4/MnO$  redox pair).

In order to favor the solid-gas reactions, the optimization of the microstructure of LSM perovskites appears as very promising way to conceive efficient catalysts for solar two-step thermochemical dissociation of  $CO_2$ . In this example, the effect of strontium substitution on the microstructure of  $LaMnO_3$  compounds was investigated.

Polycrystalline samples of  $La_{0.65}Sr_{0.35}MnO_{3-\delta}$  (LSM35),  $La_{0.50}Sr_{0.50}MnO_{3-\delta}$  (LSM50),  $La_{0.35}Sr_{0.65}MnO_{3-\delta}$  (LSM65), and  $La_{0.20}Sr_{0.80}MnO_{3-\delta}$  (LSM80) were prepared by conventional solid state method from stoichiometric  $La_2O_3$ ,  $SrCO_3$  and  $MnO_2$  powders. Phase identification was performed with powder X-ray diffraction. The XRD patterns revealed that all samples were single phase perovskites (Figure. 7).

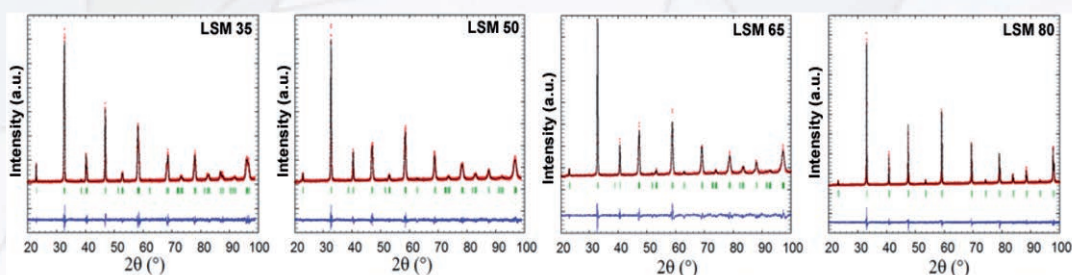


Figure 7 : LeBail fits of X-ray diffraction data collected for LSM perovskites. Experimental (red), calculated (black) and difference (blue) curves

For LSM35 to 65 compounds, variations in chemical compositions lead to distortions of the crystal lattice, modifications of the cell parameters producing perovskites superstructures of different orders. For LSM80 perovskite, a cubic symmetry was observed and used to calculate the model. The increase of the Sr content moderates the distortion present in non-substituted  $LaMnO_3$ . Ionic radius of  $Sr^{2+}$  is larger than ionic radius of  $La^{3+}$  (1.44 Å / 1.36 Å). However, the substitution of  $La^{3+}$  cations by  $Sr^{2+}$  cations is accompanied by the substitution of  $Mn^{3+}$  ions by  $Mn^{4+}$  ions. The large size difference between  $Mn^{3+}$  (0.645 Å) and  $Mn^{4+}$  (0.53 Å) ionic radius lead to a decrease of the cell volume (Figure 8).

The curve of the calculated Goldschmidt tolerance factors (GTF) follows a monotonic evolution along the LSM series. These values account for the crystal symmetry evolution within the LSM serie (Figure 9).

In summary, the LSM compounds can be clearly identified from XRD features, owing to their peak positions, crystal symmetries and cell parameter evolution with  $Sr^{2+}$  substitution for  $La^{3+}$ .

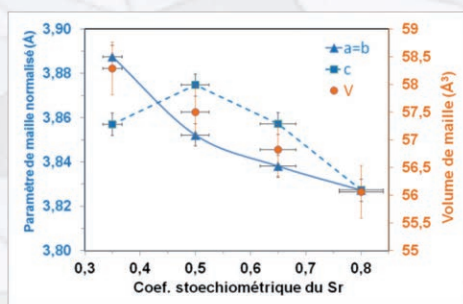


Figure 8 : Crystallographic data calculated from LeBail fits. The cell parameters were normalized from ideal cubic perovskite structure.

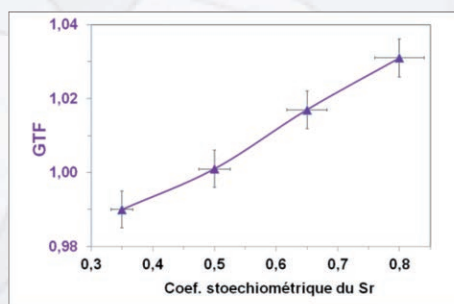


Figure 9 : Calculated Goldschmidt Tolerance Factor (GTF) of the LSM compounds.

### 2.3. Qualification of oxidized $ZrB_2$ -SiC<sub>fiber</sub> compounds elaborated at high temperature with solar energy

Permanent personnel : E. Beche, D. Perarnau, M. Balat-Pichelin (Responsable du projet)  
 Partner : V. Flaud (ICGM, Montpellier), J. Esvan, T. Duguet (ENSIACET-CIRIMAT, Toulouse), D. Sciti (ISTEC-CNR, Faenza, Italy), D. Alfano (CIRA, Capua, Italy).  
 Project : UHTC - Collaboration: SFERA grant agreement N° 228296

Catalytic recombination of dissociated atmospheric oxygen molecules on the surface of thermal protection systems (TPS) located on nose and leading edges is a significant additional heat source during the atmospheric re-entry of a space vehicle.

The challenge of the project is to qualify new candidate materials for aerospace applications. The objective of this study is to investigate the evolution of the microstructure of  $ZrB_2$ -SiC<sub>fiber</sub> compounds under critical conditions (P, T, atmosphere...)

in order to explain the surface properties and the phenomena regulating the surface oxidation of these UHTC materials.

The following composition of reference sample (A) was produced (vol%):  $ZrB_2$  + 15% SiC + 5% Si<sub>3</sub>N<sub>4</sub>. The UHTC materials were heated (1760 K (sample A1) et 2210 K (sample A2)) in the MESOX solar reactor (6 kW). SAM results confirm the nature of sample A; SiC fibers are embedded in a  $ZrB_2$  matrix (figure 10).

For the tested samples, the surfaces are fully oxidised:  $ZrO_2$  and  $SiO_2$  compounds are detected. Higher the temperature, lower the amount of silica (Figure 11). During the cooling process of samples A1 and A2, high temperature  $ZrO_2$  (tetragonal system) crystallize in monoclinic crystal system ( $T < 1430$  K).

The Coordination of the  $Zr^{4+}$  ions varies from 8 in the tetragonal phase to 7 in the monoclinic phase. Oxygen polyhedra distort to form pyramid and tetrahedron: one oxygen atom moves away (Figure 12).

The thicknesses of the protective layer of  $ZrO_2$  increase with increasing the temperature of the heating treatment (Figure 13).

At  $T=1760$  K, the surface layer was composed of a zirconia layer containing oxidized fibers. Two oxidation behaviors of SiC are detected: However, the passive oxidation is the main process ( $SiC(s) + 4O \rightarrow SiO_2(s) + CO_2(g)$ ). When the temperature increased to 2210 K, all the SiC fibers were burnt. The protective layer of zirconia contains holes and valleys corresponding to the initial SiC fibers. The main oxidation behavior of SiC is an active oxidation ( $SiC(s) + 2O \rightarrow SiO(g) + CO(g)$ ).

This study highlights the extreme complexity of UHTC oxidation behavior. Knowledge about the chemical environment on the surface and in the bulk is necessary to explain the surface properties and phenomena regulating the surface oxidation of these UHTC materials.

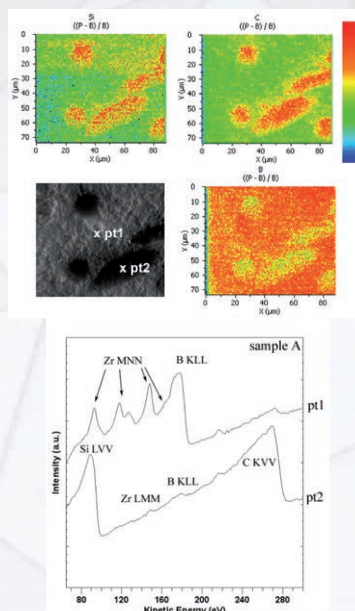


Figure 10 : Chemical information collected for reference sample (A): SAM, MEB (up), AES (down) results

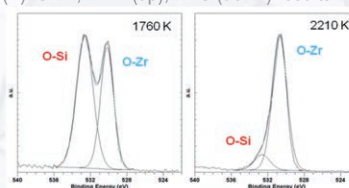


Figure 11 : O 1s XP-spectra collected for samples A1 (1760 K) and A2 (2210 K).

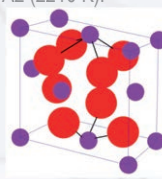


Figure 12 : Unit cell of  $ZrO_2$  (monoclinic phase): O atoms (red), Zr atoms (purple).

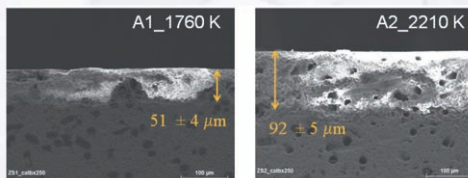


Figure 13 : SEM cross-section collected for samples A1 (1760 K) and A2 (2210 K).